ADVANCED MATERIALS
www.advmat.de

# Benchmarking to the Gold Standard: Hyaluronan-Oxime Hydrogels Recapitulate Xenograft Models with In Vitro Breast Cancer Spheroid Culture

*Alexander E. G. Baker, Laura C. Bahlmann, Roger Y. Tam, Jeffrey C. Liu, Ahil N. Ganesh, Nikolaos Mitrousis, Richard Marcellus, Melanie Spears, John M. S. Bartlett, David W. Cescon, Gary D. Bader, and Molly S. Shoichet**

**Many 3D in vitro models induce breast cancer spheroid formation; however, this alone does not recapitulate the complex in vivo phenotype. To effectively screen therapeutics, it is urgently needed to validate in vitro cancer spheroid models against the gold standard of xenografts. A new oxime-crosslinked hyaluronan (HA) hydrogel is designed, manipulating gelation rate and mechanical properties to grow breast cancer spheroids in 3D. This HA-oxime breast cancer model maintains the gene expression profile most similar to that of tumor xenografts based on a pan-cancer gene expression profile (comprising 730 genes) of three different human breast cancer subtypes compared to Matrigel or conventional 2D culture. Differences in gene expression between breast cancer cultures in HA-oxime versus Matrigel or 2D are confirmed for 12 canonical pathways by gene set variation analysis. Importantly, drug response is dependent on the culture method. Breast cancer cells respond better to the Rac inhibitor (EHT-1864) and the PI3K inhibitor (AZD6482) when cultured in HA-oxime versus Matrigel. This study demonstrates the superiority of an HA-based hydrogel as a platform for in vitro breast cancer culture of both primary, patient-derived cells and cell lines, and provides a hydrogel culture model that closely matches that in vivo.**

Despite improvements in initial target identification using computational approaches,[1] and several proposed hydrogels to culture cells for the in vitro stage of drug discovery,[2] 2D culture on tissue culture poly(styrene) (TCPS) continues to be used to screen cancer therapeutics. 2D culture does not represent the in vivo microenvironment either mechanically or biochemically, thereby leading to false positive (and likely false negative) drug hits.[3] In vivo xenograft tumor models recapitulate human disease more faithfully, but are costly, time-consuming and complicated by the use of immunocompromised mice.[4] The inaccurate but rapid and simple method of testing drugs in 2D coupled with the complexity of xenograft models, has motivated the development of more representative 3D culture platforms. A suitable 3D culture system must be sufficiently stable for drug screening and benchmarked against gold standard in vivo xenograft tumor models.[5] The limited availability of such 3D models has resulted in the continued reliance on 2D culture, even with the recognition that 2D culture does not accurately predict in vivo outcomes.

Unlike 2D culture, where breast epithelial cancer cells form a monolayer, 3D models of cancer recapitulate many disease characteristics such as formation of cancer spheroids with tight

Dr. A. E. G. Baker, L. C. Bahlmann, Dr. R. Y. Tam, Dr. J. C. Liu, Dr. A. N. Ganesh, Dr. N. Mitrousis, Prof. G. D. Bader, Prof. M. S. Shoichet
The Donnelly Centre
University of Toronto
Toronto, 160 College St, Ontario M5S 3E1, Canada
E-mail: molly.shoichet@utoronto.ca

Dr. A. E. G. Baker, Dr. R. Y. Tam, Dr. A. N. Ganesh, Prof. M. S. Shoichet
Department of Chemical Engineering and Applied Chemistry
University of Toronto
200 College Street, Toronto, Ontario M5S 3E5, Canada

Dr. A. E. G. Baker, L. C. Bahlmann, Dr. R. Y. Tam, Dr. J. C. Liu, Dr. A. N. Ganesh, Dr. N. Mitrousis, Prof. M. S. Shoichet
Institute of Biomaterials and Biomedical Engineering
164 College Street, Toronto, Ontario M5S 3G9, Canada

The ORCID identification number(s) for the author(s) of this article can be found under https://doi.org/10.1002/adma.201901166.

**DOI: 10.1002/adma.201901166**

Dr. R. Marcellus, Dr. M. Spears, Dr. J. M. S. Bartlett
Ontario Institute for Cancer Research
MaRS Centre
661 University Avenue, Toronto, Ontario M5G 0A3, Canada

Dr. M. Spears
Department of Laboratory Medicine and Pathology
University of Toronto
1 King's College Circle
Toronto, Ontario M5S 1A8, Canada

Dr. D. W. Cescon
Princess Margaret Cancer Centre
University Health Network
610 University Ave., Toronto, Ontario M5G 2C1, Canada

Prof. M. S. Shoichet
Department of Chemistry
University of Toronto
80 St. George Street, Toronto, Ontario M5S 3H6, Canada

junctions, and inclusion of key biochemical and mechanical cues of the native extracellular matrix (ECM).[6,7] Typically, cancer spheroids are formed by growing epithelial cancer cells in 3D using nonadherent conditions. This method is rapid and provides remarkable control of the spheroid size;[8] yet, unsurprisingly, the gene expression profiles of these cancer spheroids (CS) formed by aggregation resemble cells cultured in 2D more closely than those of xenograft tumors.[9] Therefore, spheroid formation alone does not recapitulate the in vivo microenvironment.[10] Nonadherent conditions lack critical ECM components, which both affect cell function through integrin-mediated signaling pathways, such as $\beta$1, and influence drug effectiveness.[11]

Laminin-rich extracellular matrices, such as Matrigel, which is derived from the Engelbreth–Holm–Swarm murine sarcoma, are favored for 3D cell culture as they contain some physiologically relevant ECM proteins that mimic the breast tumor microenvironment.[12] However, Matrigel is ill-defined,[13] and its composition, physicochemical and biomechanical properties have limited tunability.[14] Moreover, Matrigel does not include key matrix components found in the breast cancer microenvironment such as hyaluronan (HA), which is produced by tumor and stromal cells and is linked to disease progression.[15] The diversity of cell-surface integrin expression and tumor microenvironment properties across breast cancer subtypes require a model that is tunable to meet these complexities.[7,16]

The majority of chemically crosslinked hydrogels utilize chemistries that have rapid reaction kinetics,[17] such as the thiol-Michael addition ligation,[18] which can limit uniform cell encapsulation, making reproducible in vitro cell culture challenging. Moreover, many scaffold components need to be stored under inert gas due to air-sensitive functional groups, such as thiols, and/or require external stimuli to promote crosslinking, which complicates scale up.[19,20]

To achieve a more controlled system for cell encapsulation, we combined fast-reacting HA-aldehyde and slow-reacting HA-ketone with poly(ethylene glycol) (PEG)-oxyamine to create defined 3D hydrogels via oxime click chemistry. Oxime ligation is hydrolytically stable, thereby allowing long-term encapsulation of breast cancer cells—a key advance over those strategies that are inherently limited by reversible reactions, such as those that use hydrazone or Diels–Alder chemistries for crosslinking.[21,22] The oxime chemistry is insensitive to oxidation, facile to use and enables controlled gelation rates, which is often not possible with other click chemistry reactions.[19] Notwithstanding the important chemical and physical properties of these newly synthesized oxime-crosslinked HA hydrogels, our goal was not to demonstrate their superiority for 3D cell culture over other HA hydrogels, but rather to benchmark the gene expression of breast cancer cells grown in these HA-oxime hydrogels against the current gold standard of tumor xenografts grown in mice and evaluate drug response in comparison with conventional culture in 3D Matrigel and 2D TCPS (**Figure 1**a).

We synthesized HA-oxime gels with HA-ketone (HAK), HA-aldehyde (HAA), and PEG-oxyamine, each component of which first needed to be synthesized. HAK was synthesized, for the first time, in a two-step reaction: 1) amide coupling of 3-(2-methyl-1,3-dioxolan-2-yl)propan-1-amine with 4-(4,6-dimethoxy-1,3,5-triazin-2-yl)-4-methylmorpholinium chloride (DMTMM) as an activator and 2) acid-catalyzed ketone deprotection (Figure 1b). We found the substitution of ketone to be tunable between 28 ± 3% and 55 ± 2% by increasing the equivalents of DMTMM from 1.0 to 2.5, respectively (Figure S1, Supporting Information). We chose to use HAK with ≈40% ketone substitution to produce hydrogels because it was water soluble and easy to handle. Similarly, we synthesized aldehyde-modified HA (HAA) in two steps: 1) amidation of carboxylic acid groups on HA with DMTMM/aminoacetaldehyde dimethyl acetal and 2) deprotection of the resulting HA-acetal with aqueous acid (Figure 1c; Figure S2, Supporting Information). The PEG-substituted oxyamine crosslinker was prepared from either four-armed PEG-tetramine or two-armed PEG-bisamine and (boc-aminooxy)acetic acid with carbodiimide coupling followed by acid-catalyzed deprotection to yield $PEGOA_4$ and $PEGOA_2$, respectively (Figure S2, Supporting Information).

We combined HAK and HAA with $PEGOA_4$ and laminin (a common extracellular matrix protein) to produce crosslinked hydrogels with tunable biochemical properties to grow breast cancer spheroids (Figure 1d). To show that both HAK and HAA biopolymers were crosslinked with PEG-oxyamine, we compared the stability of hydrogels comprised of equal weight percent of either HAK/HAA or unmodified-HA/HAA crosslinked with PEG-oxyamine: HAK/HAA hydrogels remained stable over at least 28 days (with less than 5% decrease in mass) whereas gels formed from HA/HAA slowly dissociated, losing 50 ± 2% of their mass between day 1 and 28, reflecting the dissolution of uncrosslinked HA (Figure S3, Supporting Information). Gels crosslinked with four-armed $PEGOA_4$ swelled significantly less than those crosslinked with bifunctional $PEGOA_2$ (Figure S3, Supporting Information). Although both remained intact over four weeks, we used $PEGOA_4$ in all subsequent experiments because the increased swelling of $PEGOA_2$ crosslinked gels would alter hydrogel mechanical properties and hence cell phenotype.[23]

To achieve uniform 3D cell distribution, hydrogels must form rapidly enough to avoid cell aggregation due to gravity during gelation, but slow enough for practical use. HAA only crosslinked hydrogels (0:1, HAK:HAA) formed too quickly for cell encapsulation, requiring cells to be cultured on top of those gels versus within.[22] In contrast, hydrogels synthesized with only HAK (1:0, HAK:HAA) and $PEGOA_4$ formed too slowly, with gelation at 87 ± 11 min. Consequently, when single breast cancer cells were encapsulated in HAK-only HA-oxime gels, cells accumulated in the bottom of the well, due to the slow crosslinking reaction between ketones and oxyamines (Figure 1e). We used rheology to characterize the gelation rate of HA-oxime hydrogels with varying HAK:HAA mass ratios (Figure S4, Supporting Information). The gelation rate increased significantly with an increasing amount of HAA (Figure 1f). HA-oxime hydrogels produced with HAK:HAA mass ratios of either 7:1 or 3:1, at a constant oxyamine to ketone/aldehyde mole ratio of 0.60, resulted in mean gelation times of 35 and 25 min, respectively. At higher weight percentages of the faster gelling HAA (HAK:HAA of 1:1), the resulting crosslinked gel formed too rapidly for quantification by rheology. We used HAK:HAA of 3:1 in subsequent assays and found a uniform distribution of viable cells (Figure S5, Supporting Information). This uniform distribution was maintained for

 

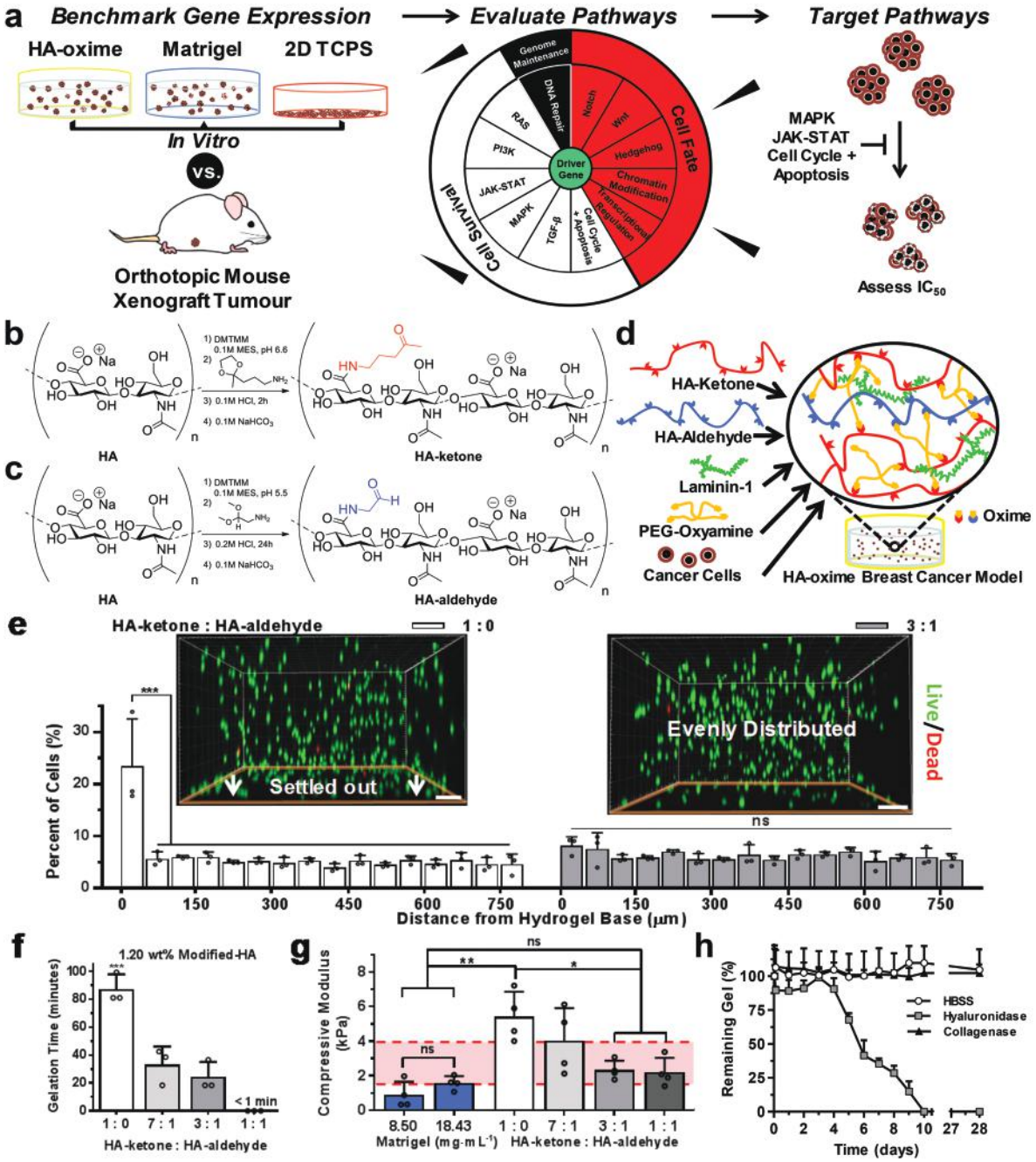


**Figure 1.** Synthesis and characterization of the HA-oxime hydrogel to model breast cancer in vitro. a) The overall goal was to benchmark the gene expression profile of cells cultured in vitro in our novel HA-oxime hydrogels relative to conventional culture in either Matrigel or 2D tissue culture polystyrene to those cells grown in vivo. This methodology allows us to identify pathways that can then be targeted in drug screening assays. b) Synthesis of HA-ketone using DMTMM coupling to HA with 3-(2-methyl-1,3-dioxolan-2-yl)propan-1-amine followed by acid-catalyzed deprotection, and neutralization. c) Synthesis of HA-aldehyde using DMTMM coupling with aminoacetaldehyde dimethyl acetal followed by acid-catalyzed deprotection, and neutralization. d) HA-oxime crosslinked hydrogels comprised of HA-ketone (red), HA-aldehyde (blue), and poly(ethylene glycol)-tetraoxyamine ($PEGOA_4$, orange) and formed in the presence of laminin (green) and breast cancer cells (tan), which resulted in uniformly distributed cells. e) Distribution of encapsulated MDA-MB-468 cells after 24 h in HA-oxime hydrogels: in HAK crosslinked gels, cells aggregate at the bottom of the well due to the slow gelation whereas in HAK:HAA (3:1 mass ratio), cells are evenly distributed. Cells were stained for viability with calcein AM (live, green) and ethidium homodimer-1 (dead, red); scale bar represents 200 μm ($n = 3$ independent experiments; mean + s.d. plotted, $^{***}p < 0.001$, one-way ANOVA, Tukey's post hoc test). f) Gelation time of HA-oxime hydrogels crosslinked with $PEGOA_4$ ($n = 3$, mean + s.d., $^{***}p < 0.001$, one-way ANOVA, Tukey's post hoc test). g) Compressive modulus of HA-oxime hydrogels compared to growth factor reduced Matrigel ($n = 4$, mean + s.d. plotted, $^{*}p < 0.05$; $^{**}p < 0.01$, one-way ANOVA, Tukey's post hoc test). The red shaded area represents the range in stiffness of mouse tumors reported in the literature.[25] h) HA-oxime hydrogel prepared from 3:1 HA-ketone (0.90 wt%) and HA-aldehyde (0.30 wt%) crosslinked with $PEGOA_4$ (1.04 wt%) was stable over 28 days at 37 °C in Hank's balanced salt solution (HBSS) and in the presence of collagenase, but degraded in the presence of hyaluronidase. The percent of remaining hydrogel was determined from the mass measurements ($n = 3$, mean + s.d. plotted).

a longer time when cells were grown in HA-oxime hydrogels versus those in Matrigel or a commercially available HA-based hydrogel, HyStem-C (HA-thiol/gelatin-thiol crosslinked with PEG diacrylate) (Figure S5c, Supporting Information).

We were interested in understanding the mechanical tunability of HA-oxime hydrogels in relation to Matrigel, the current standard for 3D cell and organoid culture. Matrigel compositions, purchased with protein concentrations of 8.50 and 18.43 mg $mL^{-1}$, had compressive moduli of 0.9 ± 0.7 and 1.6 ± 0.4 kPa, respectively, which were not significantly different from each other (Figure 1g). These formulations are typically used for in vitro culture and underscore the limited mechanical tunability offered by Matrigel.[24] In contrast, the stiffness of HA-oxime hydrogels varied with the ratio of HAK to HAA. HA-oxime hydrogels are highly tunable over 2 orders of magnitude, between 0.3 and 15 kPa, by either varying the crosslinking density or the weight percent of HA (Figure S6, Supporting Information). This range covers the stiffness reported for mouse mammary tumors (≈1.5–4.0 kPa), and human breast cancer tissue (≈5–16 kPa), as measured by compression and atomic force microscopy, respectively.[25,26]

HAK-only (1.35 wt%) hydrogels were significantly stiffer (15 ± 1 kPa) than HAA-only (1.35 wt%) hydrogels (5.5 ± 0.4 kPa) at a constant mole ratio (0.80) of oxyamine to ketone/aldehyde (Figure S6, Supporting Information). We attributed this difference in modulus of HAK-oxime and HAA-oxime hydrogels to the difference in molar mass. While we started with the same molar mass of HA, synthesis of HAK resulted in a molar mass of 311 kg $mol^{-1}$ whereas that of HAA resulted in a molar mass of 122 kg $mol^{-1}$ as measured by gel permeation chromatography. Importantly, there was no change in oxyamine to oxime conversion with all HAK and HAA formulations, as quantified by $^1$H NMR spectroscopy (Figure S7, Supporting Information), further indicating that the molar mass difference accounted for the difference in compressive modulus. The stiffness of gel formulations with 3:1 and 1:1 HAK:HAA weight ratios were not statistically different from Matrigel, so we used 3:1 ratio for future experiments as it was easier to handle. We found that these HA-oxime gels were stable for 28 days when swollen in PBS or when treated with collagenase and degraded only in the presence of hyaluronidase, highlighting the enzyme-specific degradability (Figure 1h). Importantly, breast cancer cells are known to produce hyaluronidase, which allows dynamic, cell-based spatiotemporal remodeling of the HA-oxime hydrogels during cell growth.[27]

To mimic the heterogeneity of the extracellular matrix in breast cancer and enhance cell interaction with the HA-oxime hydrogels,[28] we mixed laminin-1 (Ln) with the polymers prior to gelation and found that it was retained in the gels obviating the need for covalent immobilization: Ln incorporated at either 75 or 250 μg $mL^{-1}$ was completely retained in hydrogels after 7 days, with no soluble Ln detected in the PBS supernatant (**Figure 2**a). Given the large size of Ln (850 kDa), it was likely physically entrapped or entangled within the HA-oxime polymer chains, but may have also be retained by either (or both) electrostatic interactions between positively charged Ln and negatively charged hyaluronan-carboxylate groups[29] or reversible Schiff-base formation between basic lysine groups on laminin and HA-ketone/aldehyde groups.[30] The interactions between laminin and HA-oxime hydrogels did not alter the compressive modulus compared to HA-oxime only hydrogels thereby enabling the role of ECM proteins to be studied separately from mechanical properties (Figure S8a, Supporting Information).

To investigate cell–Ln interactions, we compared cell adhesion to HA-oxime gels with or without Ln and found more than 2-times more T47D luminal A breast cancer cells adhered to the surface of hydrogels containing 75 μg $mL^{-1}$ Ln, similar to Matrigel versus controls without Ln (Figure 2b). With or without Ln, breast cancer cells encapsulated in HA-oxime hydrogels were equally viable and evenly distributed, and the size and number of spheroids were similar (Figure S8b–i, Supporting Information). Cells within the spheroids interacted with each other, as demonstrated by E-cadherin expression, a marker of tight junctions (Figure 2c,d). Cells also interacted with the HA-oxime hydrogel through CD44, a hyaluronan receptor, and expressed $\beta$1-integrin, a Ln receptor (Figure 2e–h). CD44 is essential to the growth of breast cancer cells and $\beta$1-integrin is involved in the PI3K pathway, which is upregulated in breast cancer and constitutes a drug target (Figure S9, Supporting Information).[31] Given the relevance of hyaluronan in breast cancer[32] and the interaction of cells with the HA-oxime hydrogels, we wondered whether culture in HA-oxime with or without laminin would impact the gene expression levels compared to those in Matrigel and conventional 2D TCPS.

When cells from five different breast cancer cell lines were cultured for 21 days in HA-oxime hydrogels ± Ln they formed spheroids, which was not observed in 2D culture (Figure S10, Supporting Information). These cells represent 4 breast cancer subtypes with different expression profiles of estrogen receptor (ER), progesterone receptor (PR), and human epidermal growth factor receptor 2 (HER2): luminal A MCF7 and T47D ($ER^+$, $PR^+$, and $HER2^-$), luminal B BT474 ($ER^+$, $PR^+$, and $HER2^+$), HER2-overexpressing MDA-MB-231-H2N ($ER^-$, $PR^-$, and $HER2^+$), and triple negative MDA-MB-468 ($ER^-$, $PR^-$, and $HER2^-$) cells. By examining proliferation in 2D and 3D, and between different hydrogel cultures, we observed that all breast cancer cell lines exhibited similar proliferation rates in HA-oxime ± Ln hydrogels compared to Matrigel except BT474 cells, where proliferation was increased in Matrigel (**Figure 3**a). In addition, the HA-oxime hydrogels enable oxygen and nutrient penetration based on the presence of cancer spheroids throughout the thickness of the hydrogels (Figure S11, Supporting Information). In all cases cells formed spheroids in HA-oxime and Matrigel at 21 days (Figure 3b), indicating phenotypic equivalence at minimum.

Recent efforts to develop in vitro cancer models that recapitulate the features of human breast cancer for preclinical testing or personalized medicine have used poorly defined Matrigel to grow 3D tumor organoids. To test the HA-oxime hydrogel for these applications, we encapsulated patient-derived primary luminal B breast cancer cells in 3D therein and observed their survival and proliferation: the patient-derived cells grew as spheroids in the hydrogel but proliferated as monolayers on 2D TCPS (Figure S12, Supporting Information). Impressively, encapsulated primary breast cancer cells from a dissociated patient biopsy formed spheroids in both HA-oxime ± Ln and Matrigel after 21 days of culture (Figure 3c–f). It is possible

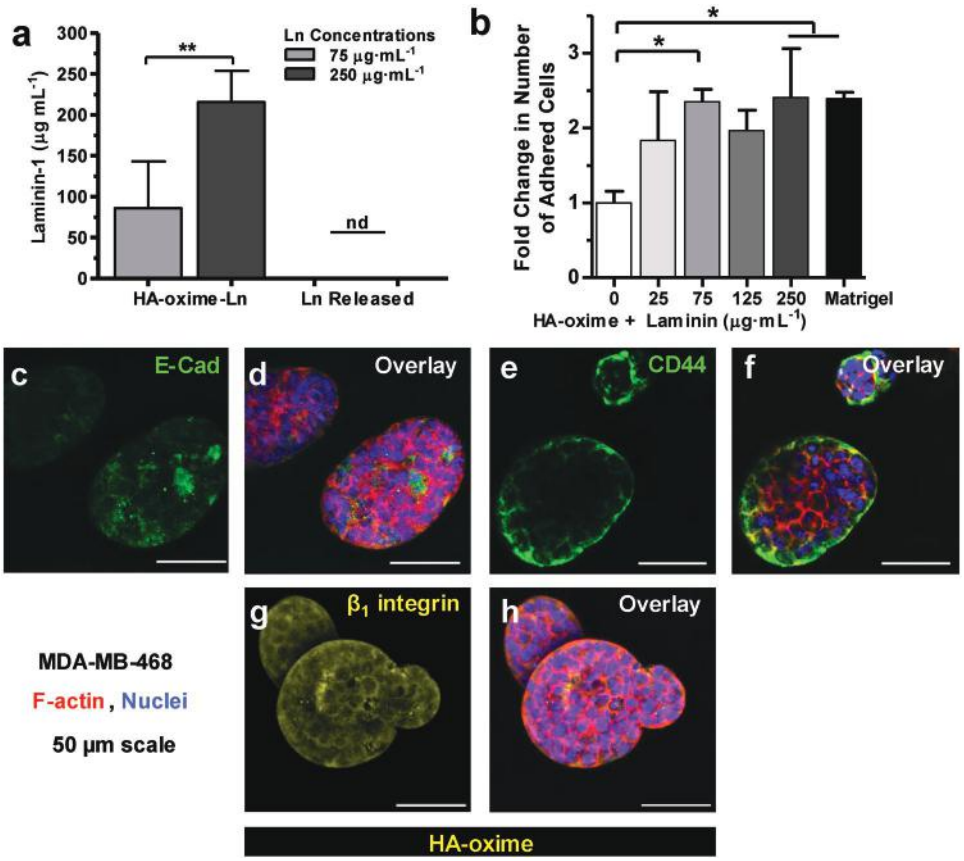


**Figure 2.** Impact of laminin in HA-oxime hydrogels. a) The amount of Ln retained in HA-oxime hydrogels crosslinked with $PEGOA_4$ quantified by ELISA after 7 days, Ln was not detected (nd) from supernatant 24 h after adding PBS to HA-oxime-Ln hydrogels ($n = 3$ independent samples; mean + standard deviation plotted, no significant differences (ns), $^{**}p < 0.01$, one-way ANOVA, Tukey's post hoc test). b) Fold change in the number of breast cancer cells on HA-oxime gels crosslinked with $PEGOA_4$ containing Ln versus those on Matrigel ($n = 3$ independent studies; mean + standard deviation plotted, $^{*}p < 0.05$; one-way ANOVA, Tukey's post hoc test). c–h) Representative immunocytochemistry images of MDA-MB-468 cells encapsulated in HA-oxime hydrogels after 21 days stained for nuclei (with Hoechst, blue) and actin (with phalloidin which binds to F-actin, red): c,d) E-cadherin, e,f) CD44, and g,h) $\beta_1$ integrin.

that over the 21 days of culture within the 3D hydrogel, glucose and/or oxygen gradients will form and result in heterogeneity that more closely mimics the tumor microenvironment within the xenograft versus that of 2D TCPS. These results led us to perform a more extensive comparison of gene expression between the mouse xenografts and in vitro models in order to better understand the biological differences between these in vitro models.

In order to understand how breast cancer markers and drug-targetable pathways are impacted by culture platform, we benchmarked the gene expression of five cell lines cultured in HA-oxime ± Ln against orthotopic mouse xenografts in NOD SCID gamma mice and compared them to those in Matrigel or 2D TCPS (Figures S13 and S14, Supporting Information). In general, the gene expression of breast cancer cells cultured in either HA-oxime hydrogels ± Ln or Matrigel were more similar to that of mouse xenograft models than cells cultured on 2D TCPS (Figure 3g). Several genes were differentially expressed compared to tumor xenografts when cultured on 2D TCPS, but not when cultured in HA-oxime hydrogels, including epidermal growth factor receptor (EGFR), human epidermal growth factor receptor 2 (ERBB2) and phosphatidylinositol-4,5-bisphosphate 3-kinase catalytic subunit alpha (PIK3CA) which are implicated in drug targetable pathways (Table S1, Supporting Information). The expression of both ERBB2 and EGFR can result in changes to cell phenotype and tumorigenicity, and may also influence response to therapy, including agents targeting these receptors directly.[33] In addition, patients with PIK3CA-positive breast tumors have shorter disease-free survival across all molecular subtypes indicating its potential as a therapeutic target.[34] Thus, these results further underscore the need to use representative 3D models to study breast cancer over traditional 2D culture.

A potential strategy for treating breast cancer beyond traditional kinase inhibitors includes emerging metabolic targets such as FASN, which is responsible for lipid synthesis. Currently, the FASN inhibitor TVB-2640 is being evaluated for the treatment of advanced breast cancer in a clinical trial.[35] Due to observed differences in cellular fatty acid and cholesterol content between 2D culture and xenograft models,[36] we hypothesized that the expression of lipid metabolic genes would be more similar in 3D cell culture than 2D culture relative to the xenograft tumors. The expression of FASN, which is responsible for lipid synthesis, and ATP-binding cassette transporter (ABCA1), which regulates intracellular phospholipid and cholesterol homeostasis, depended upon both cell line and culture system. For example,

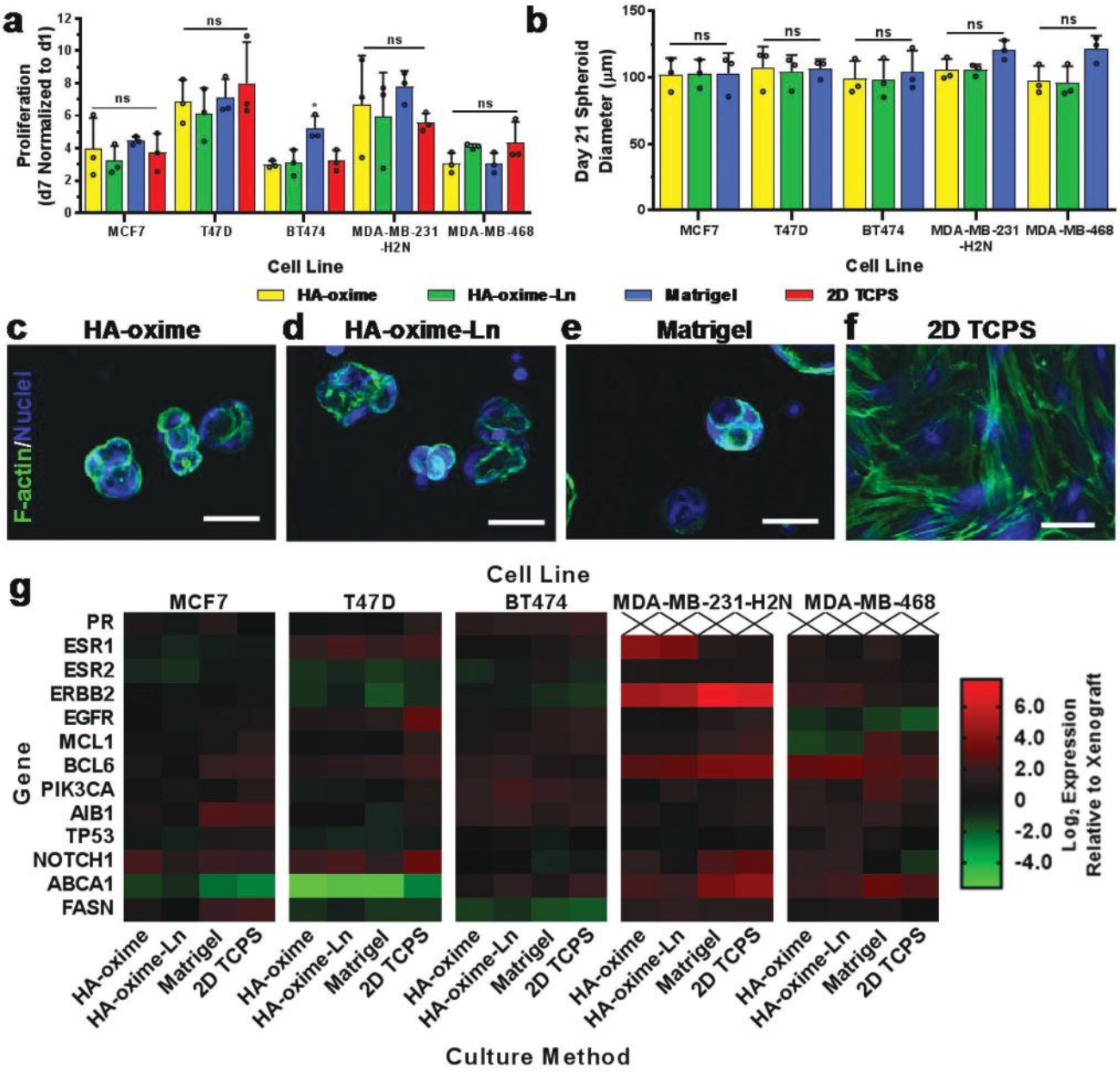


**Figure 3.** Evaluation of patient-derived and five different breast cancer cell lines in HA-oxime ± Ln versus Matrigel and 2D TCPS. a) Cell growth at day 7 relative to day 1 ($n = 3$; mean + s.d. plotted, $*p < 0.05$, one-way ANOVA, Tukey's post hoc test). b) Tumor spheroid diameter after 21 days of culture for cells embedded in HA-oxime, HA-oxime-Ln or Matrigel ($n = 3$; mean + s.d. plotted, $*p < 0.05$, one-way ANOVA, Tukey's post hoc test). No spheroids were formed on 2D TCPS. c–f) Representative images of primary, patient breast cancer cells after 21 days of culture in HA-oxime (c), HA-oxime + Ln (d), Matrigel (e), or 2D TCPS (f). Cells stained with phalloidin (binds to F-actin, shown in green) and Hoechst (nuclei, shown in blue); scale bar represents 50 μm. g) Heat map gene expression of MCF7, T47D, BT474, MDA-MB-231-H2N, and MDA-MB-468 cells encapsulated in HA-oxime, HA-oxime-Ln, Matrigel, or cultured on 2D TCPS after 21 days and compared to the respective mouse xenograft tumors. Expression reported as the $Log_2$ ratio from qPCR with black indicating the greatest similarity ($n = 3$–5 independent studies; mean plotted).

luminal A MCF7 cells had similar ABCA1 and FASN expression between tumor xenograft and HA-oxime hydrogel culture, but an upregulated FASN expression when cultured on 2D TCPS or Matrigel (Figure 3g). This shows that FASN expression is influenced by the ECM and that gene expression levels of xenograft tumors for luminal A breast cancer were recapitulated using the HA-oxime hydrogel. However, HER2-overexpressing MDA-MB-231-H2N cells upregulated FASN and ABCA1 across all in vitro models, which suggests altered lipid metabolism and secretion compared to xenograft tumors. These differences in FASN expression were not observed for other breast cancer subtypes, which supports breast cancer subtype-dependent lipid metabolism in 2D.[37] Considering the similar gene expression of breast cancer cells cultured in HA-oxime hydrogels and grown as

xenograft tumors, we performed more rigorous benchmarking with a pan-cancer gene expression panel.

In order to better understand the predictive powers of 3D in vitro culture of breast cancer cells, we benchmarked three distinct cell lines, representing three different breast cancer subtypes, to tumor xenografts: luminal B (BT474); HER2-overexpressing (MDA-MB-231-H2N); and triple negative (MDA-MB-468). We cultured cells in 3D in HA-oxime, Matrigel or in 2D on TCPS and compared the gene expression panel of 730 cancer-related genes. Relative to tumor xenografts, we found that luminal B, BT474 cells had the fewest number of differentially expressed genes when cultured in HA-oxime gels (24 downregulated and 27 upregulated of 730 genes) compared to those cultured in Matrigel (63 downregulated and 135 upregulated) and on 2D TCPS (60 downregulated, 45 upregulated) (**Figure 4**a,b; Table S2, Supporting Information). Surprisingly, there were more differences when cells were cultured in Matrigel than on 2D TCPS relative to xenografts, which both reflects the unsuitability of Matrigel and demonstrates that 3D culture alone is insufficient for predictive drug screening.

We analyzed 12 pathways and driver genes by gene set variation analysis and found that BT474 cells cultured in Matrigel altered the expression of several pathways including JAK-STAT and MAPK versus tumor xenografts whereas cells cultured in HA-oxime gels did not (Figure 4c). This further motivates the use of representative, benchmarked 3D in vitro models, such as the HA-oxime hydrogel, to recapitulate gene expression and to evaluate new drug candidates against JAK-STAT and MAPK.[38]

Comparing the gene expression of MDA-MB-231-H2N tumors to 3D hydrogels and 2D culture, we found that fewer genes were differentially expressed when cells were grown in HA-oxime gels (16 downregulated, 12 upregulated) versus both Matrigel (28 downregulated, 21 upregulated) and 2D TCPS (33 downregulated, 29 upregulated) (Figure 4d,e; Table S3, Supporting Information). Altered gene expression of a therapeutic target in cells used in an in vitro drug screen would generate misleading data. Differences in the JAK-STAT pathway were identified between cells cultured in HA-oxime, Matrigel or 2D TCPS relative to the tumor xenografts after analyzing the pathways regulating cell survival and cell fate between the in vitro models and tumor xenografts of MDA-MB-231-H2N cells (Figure 4f).

When triple-negative breast cancer (TNBC) MDA-MB-468 cells were cultured in HA-oxime gels, Matrigel or 2D TCPS, a similar number of genes were downregulated compared to the xenograft tumors (125, 134, and 122, respectively) while the number of upregulated genes was higher in 2D TCPS (94) versus HA-oxime and Matrigel (60 and 54 genes, respectively) (Figure 4g,h; Table S4, Supporting Information). Subsequent analysis of affected pathways revealed that the hedgehog pathway was altered when cultured in HA-oxime, Matrigel, or 2D TCPS relative to the tumor xenografts (Figure 4i). Since only 30% of triple-negative breast cancers involve paracrine hedgehog (Hh) signaling, which has been studied in the context of cancer-associated fibroblasts, coculture models may be required to target this pathway.[39]

Our gene expression pathway analyses show that the JAK-STAT pathway was altered in both $HER2^+$ BT474 and MDA-MB-231-H2N cell lines when cultured in Matrigel or on 2D TCPS relative to xenograft and HA-oxime. This underlines the need to evaluate drugs targeting specific pathways on validated models. Remarkably, while Matrigel is thought to be the gold standard for in vitro culture, it has not been benchmarked previously and our data clearly demonstrate that it is suboptimal. Overall, HA-oxime gels were the most similar to xenografts, with only 294 differentially expressed genes versus 434 for Matrigel and 371 for 2D TCPS (Figure 4j; Figure S15, Supporting Information). The number of differentially expressed genes for the same cell lines was similar between HA-oxime and HA-oxime-Ln hydrogels (294 vs 308 genes, respectively) compared to the xenograft tumors (Figure S15b, Supporting Information). Thus, 3D culture reduces, but does not eliminate, differences in gene expression between 2D culture and xenografts. 3D culture in HA-oxime better emulates the gene expression profile of xenografts than culture in Matrigel.

To understand if these differences in gene expression could influence cell response in drug screening, we specifically chose drugs that target pathways differentially expressed between xenograft and in vitro culture in Matrigel and 2D TCPS and that were not differentially expressed in HA-oxime (Tables S4 and S5, Supporting Information). We tested a series of drugs that target the MAPK (such as Rac signaling) and JAK-STAT pathways of BT474 cells grown in HA-oxime versus Matrigel and 2D TCPS.

BT474 cells treated with EHT-1864 (Rac inhibitor, targeting the MAPK/ERK pathway) were more responsive when cultured in HA-oxime than in Matrigel (**Figure 5**a; Figure S16, Supporting Information). In addition, BT474 cells cultured in HA-oxime were more responsive to AZD6482 (PI3K$\beta$ inhibitor involved in the JAK-STAT pathway) than those cultured in Matrigel or on 2D TCPS (Figure 5b). To gain biological insight into the mechanism underlying the observed differences in drug responsiveness, we quantified the number of genes involved in MAPK and JAK-STAT signaling pathways with differential expression levels relative to tumor xenografts: cells cultured in HA-oxime had fewer differentially expressed genes (14 for MAPK and 4 for JAK-STAT) compared to cells cultured in both Matrigel (43 for MAPK and 29 for JAK-STAT) and on 2D TCPS (23 for MAPK and 10 for JAK-STAT) (Figure 5c–e; red circles for MAPK and green circles for JAK-STAT). Together these results demonstrate the superiority of HA-oxime over Matrigel and 2D TCPS in drug screening where specific pathways are targeted.

Interestingly, cells cultured in HA-oxime were over ten-fold more sensitive to maritoclax (Figure S16c, Supporting Information), an Mcl-1 inhibitor which prevents the normal antiapoptotic signaling by Mcl-1 on the mitochondria resulting in apoptosis, with an $IC_{50}$ of $0.59 \times 10^{-6}$ M than those cultured in 2D TCPS with $IC_{50}$ of $5.5 \times 10^{-6}$ M (Figure 5f). Moreover, primary, human patient tumor luminal B breast cancer cells were significantly more sensitive to maritoclax when cultured in 3D HA-oxime than those cultured on 2D TCPS as well, demonstrating both the potential of the HA-oxime hydrogels in personalized medicine and the importance of culture conditions in drug screening (Figure S17, Supporting Information). Maritoclax targets the apoptosis pathway as an inhibitor of antiapoptotic protein Mcl-1 on the mitochondria. Regulators of this apoptosis pathway, BAD (proapoptotic) and BCL2

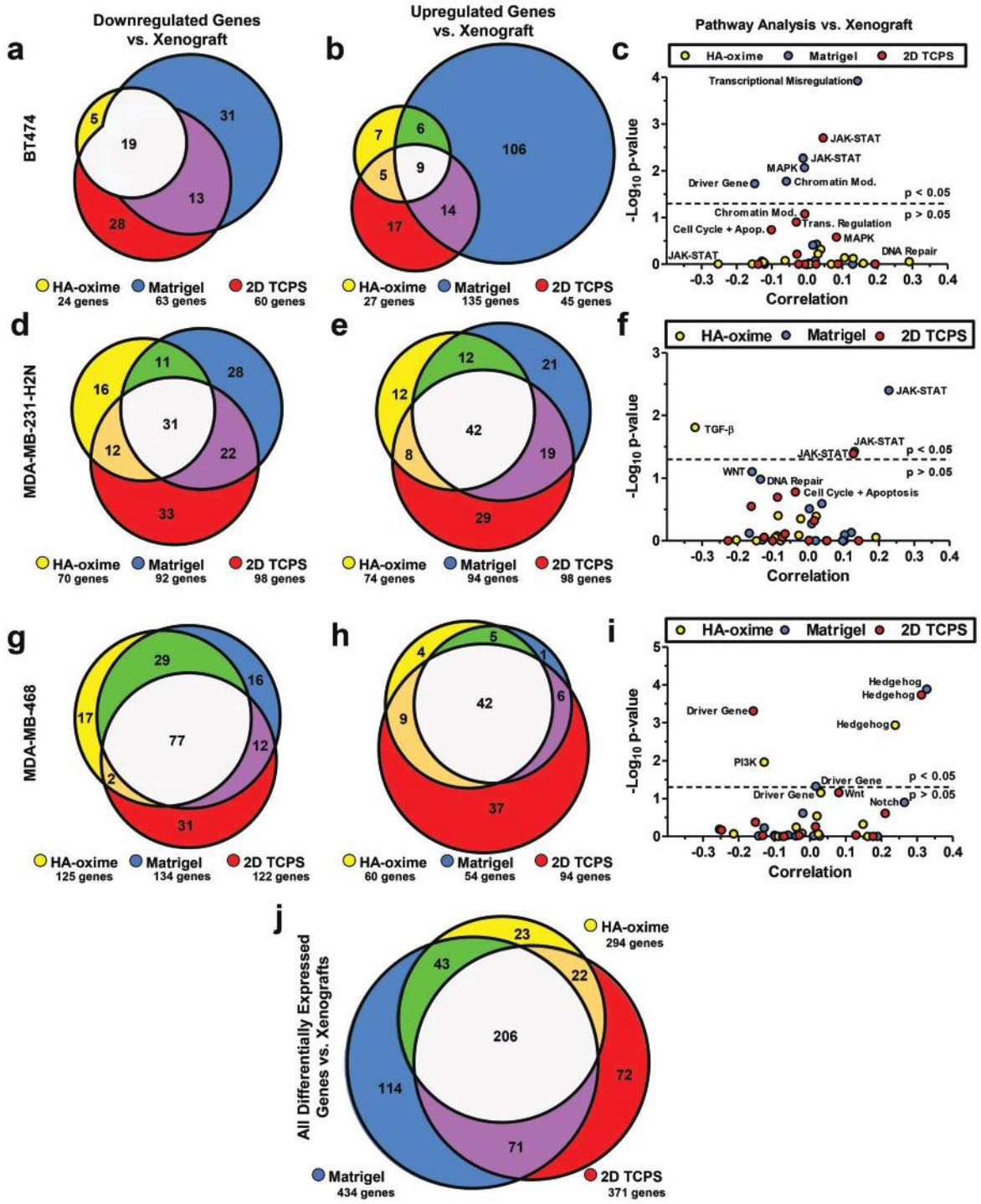


**Figure 4.** Comparison of in vitro gene expression and pathway analysis for three breast cancer cell lines relative to tumor xenografts in mice. a,b) Venn diagrams depicting the number genes differentially expressed by BT474 cells cultured in vitro compared to xenografts. c) Pathway specific expression correlation values and *p*-values by gene set variation analysis of BT474 cells cultured in vitro versus tumor xenografts. Altered pathways in cells cultured in vitro are shown above the dashed line. d,e) Venn diagrams depicting the number genes differentially expressed by MDA-MB-231-H2N cells cultured in vitro compared to xenografts. f) Pathway specific expression correlation values and *p*-values by gene set variation analysis of MDA-MB-231-H2N cells cultured in vitro versus tumor xenografts. Altered pathways in cells cultured in vitro are shown above the dashed line. g,h) Venn diagrams depicting the number of genes differentially expressed by MDA-MB-468 cells cultured in vitro compared to xenografts. i) Pathway specific expression correlation values and *p*-values by gene set variation analysis of MDA-MB-468 cells cultured in vitro versus tumor xenografts. Altered pathways in cells cultured in vitro are shown above the dashed line. Pathway specific expression correlation values and *p*-values by gene set variation analysis versus tumor xenografts. j) Summary of all observed differentially expressed genes after culture in HA-oxime, Matrigel, or 2D TCPS versus mouse xenograft tumors for BT474, MDA-MB-231-H2N, and MDA-MB-468 cells ($n = 3$ except for BT474 cells grown in Matrigel where $n = 4$).

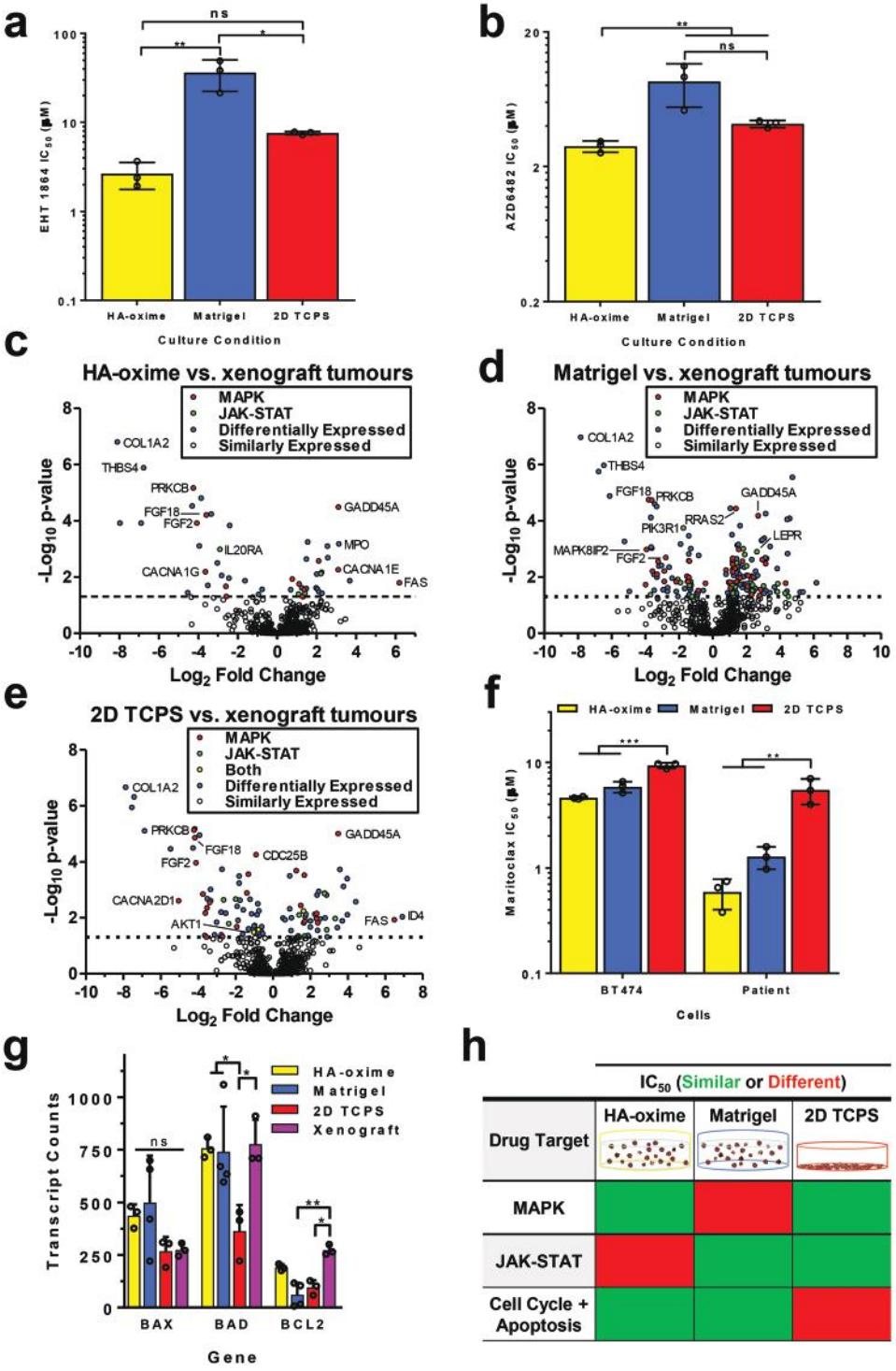


**Figure 5.** Targeting pathways in BT474 breast cancer cells cultured in vitro with drugs. a,b) $IC_{50}$ values for BT474 cells cultured in vitro treated with a) EHT 1864 targeting the MAPK pathway or b) AZD6482 targeting the JAK-STAT pathway ($n = 3$ independent experiments; mean + standard deviation plotted, $*p < 0.05$, $**p < 0.01$, by one-way ANOVA, Tukey's post hoc test). c–e) Volcano plots of differentially expressed genes involved in MAPK signaling (red), JAK-STAT signaling (green), both pathways (yellow), other (blue) and similarly expressed (white) when cultured in HA-oxime (c), Matrigel (d), or on 2D TCPS (e) versus tumor xenografts. f) $IC_{50}$ values for BT474 and patient derived breast cancer cells cultured in vitro treated with maritoclax targeting the apoptosis pathway ($n = 3$ independent experiments; mean + standard deviation plotted, $**p < 0.01$, $***p < 0.001$ by one-way ANOVA, Tukey's post hoc test). g) Gene expression counts of apoptosis signaling genes BAX, BAD, and BCL2 for BT474 cells cultured in vitro or as tumor xenografts. h) Summary of observed statistical differences in $IC_{50}$ values from drug screening with EHT 1864 (which targets MAPK), AZD6482 (which targets JAK-STAT) and maritoclax (which targets apoptosis) with BT474 cells cultured in HA-oxime, Matrigel or on 2D TCPS. $IC_{50}$ values that were statistically different depending on culture platform are shown in red while those which were not statistically different are shown in green.

(antiapoptotic), had decreased levels in BT474 cells cultured on 2D TCPS relative to 3D culture, which explains the observed differences in drug response (Figure 5g).

We highlight the results of the in vitro drug screening performed with BT474 cells where $IC_{50}$ values differed between HA-oxime, Matrigel and 2D TCPS (Figure 5h). Since the decision to test drugs in animal models of disease is often based on in vitro screening, maritoclax, EHT-1864 and AZD6482 would have been excluded based on culture in Matrigel and/or 2D TCPS, thereby reflecting the importance of culture in a representative matrix, such as HA-oxime. The differences between 2D and 3D culture of breast cancer cells are significant in terms of gene expression and drug response. While cell response did not always differ between the 3 culture conditions (as shown with ZSTK474 and afatinib; Figure S16, Supporting Information), to ensure comprehensive screening, a validated, representative system, like HA-oxime, is required.

To gain insight into the broader utility of the HA-oxime hydrogels with other cell types, we investigated the efficacy of erlotinib, an EGFR inhibitor, against TNBC MDA-MB-468 cells. Cells that were grown on 2D TCPS, in Matrigel or HA-oxime for 21 days and treated with erlotinib for 7 days had a significantly higher $IC_{50}$ of $37.6 \times 10^{-6}$ M ($p < 0.01$) compared to those cultured in 3D of $\approx 4.5 \times 10^{-6}$ M (Figure S18, Supporting Information). MDA-MB-468 cells cultured on 2D were less sensitive to erlotinib than other cancer cell lines, despite its established effectiveness in breast cancer xenografts in mice,[40] further highlighting the importance of relevant screening assays.

3D cell culture has several features which make it attractive for drug screening, yet is limited by the use of Matrigel, which does not faithfully recapitulate the gene expression profile of the tumor xenograft and is chemically ill-defined. The newly synthesized HA-oxime hydrogels have controlled and tunable gelation, mechanical properties, and chemical properties that mimic the breast ECM, which are not possible with 2D TCPS and limited with Matrigel. By benchmarking to the in vivo gold standard for the first time, we demonstrate that breast cancer cells grown in HA-oxime hydrogels most closely resemble orthotopic xenografts in terms of gene expression profiles of three distinct breast cancer subtypes. This impacts the value of in vitro drug screening. Formulating the HA-oxime hydrogels with laminin did not reduce the number of differentially expressed genes expressed by the breast cancer spheroids compared to the tumor xenografts. Our analysis of canonical signaling pathways using the gene expression data suggest breast cancer subtype-dependent changes to gene expression with culture platform. We demonstrated the ability to grow patient-derived breast cancer cells in HA-oxime hydrogels and thereby identify relevant drug candidates. Thus, hyaluronan-oxime hydrogels bridge the gap between 2D drug screening in vitro and in vivo mouse xenograft models, opening the door to personalized medicine and more predictive drug screening. To take full advantage of this opportunity, scale up and simultaneous screening of multiple drugs is required. This well-defined hydrogel platform opens up the possibility for more complex 3D models with coculture of multiple cell types, thereby better emulating the complexity of tumors. Moreover, given the benefit in vitro, we postulate that these HA-oxime hydrogels could displace Matrigel to facilitate tumor engraftment in vivo as well.

## Experimental Section

Detailed methods are presented in the Supplementary Information.

## Supporting Information

Supporting Information is available from the Wiley Online Library or from the author.

## Acknowledgements

The authors are grateful for funding from the Natural Sciences and Engineering Research Council of Canada (Discovery grant to M.S.S., CGSD to A.E.G.B. and L.C.B., and PGSD to A.N.G.) and the Canadian Institute for Health Research (Foundation grant to M.S.S.). The authors acknowledge the Canadian Foundation for Innovation, project number 19119, and the Ontario Research Fund for funding of the Centre for Spectroscopic Investigation of Complex Organic Molecules and Polymers. The authors also thank to Dr. Robert Kerbel (Sunnybrook Health Science Centre) for generously providing us with the MDA-MB-231-H2N cell line; members of the Shoichet Lab for thoughtful review of this paper; Laura Smith for the synthesis of monofunctional HA-methylfuran; and Sarah Chagri, Tobias Bauer, and Erik Kersten for their contributions. Patient breast cancer cells were obtained commercially or under University Health Network Research Ethics Board protocol #06-0196 from Princess Margaret Cancer Centre in Toronto, ON, Canada. All animal studies were performed in accordance with an approved protocol by the University Health Network Animal Care Committee under the guidelines of the Canadian Council on Animal Care.

## Conflict of Interest

The authors declare no conflict of interest.

## Keywords

3D cell culture, breast cancer, drug screening, hyaluronic acid, hydrogels

Received: February 19, 2019
Revised: June 28, 2019
Published online:

[1] a) S. P. Leelananda, S. Lindert, *Beilstein J. Org. Chem.* **2016**, *12*, 2694; b) V. Malik, J. K. Dhanjal, A. Kumari, N. Radhakrishnan, K. Singh, D. Sundar, *Methods* **2017**, *131*, 10.
[2] Y. Li, E. Kumacheva, *Sci. Adv.* **2018**, *4*, eaas899.
[3] N. Jacobi, R. Seeboeck, E. Hofmann, H. Schweiger, V. Smolinska, T. Mohr, A. Boyer, W. Sommergruber, P. Lechner, C. Pichler-Huebsc hmann, K. Onder, H. Hundsberger, C. Wiesner, A. Eger, *Oncotarget* **2017**, *8*, 107423.
[4] T. Hasan, B. Carter, N. Denic, L. Gai, J. Power, K. Voisey, K. R. Kao, *J. Clin. Pathol.* **2015**, *68*, 746.
[5] C.-P. Day, G. Merlino, T. Van Dyke, *Cell* **2015**, *163*, 39.
[6] a) A. Ivascu, M. Kubbies, *Int. J. Oncol.* **2007**, *31*, 1403; b) Y. Imamura, T. Mukohara, Y. Shimono, Y. Funakoshi, N. Chayahara, M. Toyoda, N. Kiyota, S. Takao, S. Kono, T. Nakatsura, H. Minami, *Oncol. Rep.* **2015**, *33*, 1837.
[7] J. R. Todd, K. A. Ryall, S. Vyse, J. P. Wong, R. C. Natrajan, Y. Yuan, A.-C. Tan, P. H. Huang, *Oncotarget* **2016**, *7*, 62939.

 

[8] F. Madoux, A. Tanner, M. Vessels, L. Willetts, S. Hou, L. Scampavia, T. P. Spicer, *SLAS Discovery* **2017**, *22*, 516.
[9] E. R. Boghaert, X. Lu, P. E. Hessler, T. P. McGonigal, A. Oleksijew, M. J. Mitten, K. Foster-Duke, J. A. Hickson, V. E. Santo, C. Brito, T. Uziel, K. S. Vaidya, *Neoplasia* **2017**, *19*, 695.
[10] a) J. E. Sero, H. Z. Sailem, R. C. Ardy, H. Almuttaqi, T. Zhang, C. Bakal, *Mol. Syst. Biol.* **2015**, *11*, 790; b) M. F. Gencoglu, L. E. Barney, C. L. Hall, E. A. Brooks, A. D. Schwartz, D. C. Corbett, K. R. Stevens, S. R. Peyton, *ACS Biomater. Sci. Eng.* **2018**, *4*, 410.
[11] a) R. Xu, J.-H. Mao, *Integr. Biol.* **2011**, *3*, 368; b) C. J. Lovitt, T. B. Shelper, V. M. Avery, *BMC Cancer* **2018**, *18*, 41.
[12] B. Weigelt, C. M. Ghajar, M. J. Bissell, *Adv. Drug Delivery Rev.* **2014**, *69–70*, 42.
[13] C. S. Hughes, L. M. Postovit, G. A. Lajoie, *Proteomics* **2010**, *10*, 1886.
[14] L. Lambricht, P. De Berdt, J. Vanacker, J. Leprince, A. Diogenes, H. Goldansaz, C. Bouzin, V. Préat, C. Dupont-Gillain, A. d. Rieux, *Dent. Mater.* **2014**, *30*, e349.
[15] P. Auvinen, R. Tammi, J. Parkkinen, M. Tammi, U. Agren, R. Johansson, P. Hirvikoski, M. Eskelinen, V. M. Kosma, *Am. J. Pathol.* **2000**, *156*, 529.
[16] A. Rizwan, M. Cheng, Z. M. Bhujwalla, B. Krishnamachary, L. Jiang, K. Glunde, *npj Breast Cancer* **2015**, *1*, 15017.
[17] H. Wang, D. Zhu, A. Paul, L. Cai, A. Enejder, F. Yang, S. C. Heilshorn, *Adv. Funct. Mater.* **2017**, *27*, 1605609.
[18] F. Saito, H. Noda, J. W. Bode, *ACS Chem. Biol.* **2015**, *10*, 1026.
[19] S. A. Fisher, A. E. G. Baker, M. S. Shoichet, *J. Am. Chem. Soc.* **2017**, *139*, 7416.
[20] A. K. Jha, K. M. Tharp, S. Browne, J. Ye, A. Stahl, Y. Yeghiazarians, K. E. Healy, *Biomaterials* **2016**, *89*, 136.
[21] a) J. Kalia, R. T. Raines, *Angew. Chem., Int. Ed.* **2008**, *47*, 7523; b) C. Kascholke, T. Loth, C. Kohn-Polster, S. Möller, P. Bellstedt, M. Schulz-Siegmund, M. Schnabelrauch, M. C. Hacker, *Biomacromolecules* **2017**, *18*, 683.
[22] A. E. G. Baker, R. Y. Tam, M. S. Shoichet, *Biomacromolecules* **2017**, *18*, 4373.
[23] H.-H. Lin, H.-K. Lin, I. H. Lin, Y.-W. Chiou, H.-W. Chen, C.-Y. Liu, H. I. C. Harn, W.-T. Chiu, Y.-K. Wang, M.-R. Shen, M.-J. Tang, *Oncotarget* **2015**, *6*, 20946.
[24] M. Smolina, E. Goormaghtigh, *Analyst* **2016**, *141*, 620.
[25] M. J. Paszek, N. Zahir, K. R. Johnson, J. N. Lakins, G. I. Rozenberg, A. Gefen, C. A. Reinhart-King, S. S. Margulies, M. Dembo, D. Boettiger, D. A. Hammer, V. M. Weaver, *Cancer Cell* **2005**, *8*, 241.
[26] a) K. R. Levental, H. Yu, L. Kass, J. N. Lakins, M. Egeblad, J. T. Erler, S. F. T. Fong, K. Csiszar, A. Giaccia, W. Weninger, M. Yamauchi, D. L. Gasser, V. M. Weaver, *Cell* **2009**, *139*, 891; b) A. Ansardamavandi, M. Tafazzoli-Shadpour, R. Omidvar, I. Jahanzad, *J. Mech. Behav. Biomed. Mater.* **2016**, *60*, 234.
[27] a) L. Edjekouane, S. Benhadjeba, M. Jangal, H. Fleury, N. Gévry, E. Carmona, A. Tremblay, *Oncotarget* **2016**, *7*, 77276; b) H. Tan, H. Li, J. P. Rubin, K. G. Marra, *J. Tissue Eng. Regener. Med.* **2011**, *5*, 790.
[28] a) A. S. Caldwell, G. T. Campbell, K. M. T. Shekiro, K. S. Anseth, *Adv. Healthcare Mater.* **2017**, *6*, 1700254; b) S. Suri, C. E. Schmidt, *Tissue Eng., Part A* **2010**, *16*, 1703; c) Z.-N. Zhang, B. C. Freitas, H. Qian, J. Lux, A. Acab, C. A. Trujillo, R. H. Herai, V. A. Nguyen Huu, J. H. Wen, S. Joshi-Barr, J. V. Karpiak, A. J. Engler, X.-D. Fu, A. R. Muotri, A. Almutairi, *Proc. Natl. Acad. Sci. USA* **2016**, *113*, 3185.
[29] M. Rinaudo, *Int. J. Biol. Macromol.* **2008**, *43*, 444.
[30] S. E. Stabenfeldt, A. J. Garcia, M. C. LaPlaca, *J. Biomed. Mater. Res., Part A* **2006**, *77A*, 718.
[31] a) S. Godar, T. A. Ince, G. W. Bell, D. Feldser, J. L. Donaher, J. Bergh, A. Liu, K. Miu, R. S. Watnick, F. Reinhardt, S. S. McAllister, T. Jacks, R. A. Weinberg, *Cell* **2008**, *134*, 62; b) K. To, A. Fotovati, K. M. Reipas, J. H. Law, K. Hu, J. Wang, A. Astanehe, A. H. Davies, L. Lee, A. L. Stratford, A. Raouf, P. Johnson, I. M. Berquin, H. D. Royer, C. J. Eaves, S. E. Dunn, *Cancer Res.* **2010**, *70*, 2840; c) R. Castello-Cros, D. R. Khan, J. Simons, M. Valianou, E. Cukierman, *BMC Cancer* **2009**, *9*, 94.
[32] a) P. Heldin, K. Basu, B. Olofsson, H. Porsch, I. Kozlova, K. Kahata, *J. Biochem.* **2013**, *154*, 395; b) P. Auvinen, R. Tammi, V.-M. Kosma, R. Sironen, Y. Soini, A. Mannermaa, R. Tumelius, E. Uljas, M. Tammi, *Int. J. Cancer* **2013**, *132*, 531.
[33] S. Ingthorsson, K. Andersen, B. Hilmarsdottir, G. M. Maelandsmo, M. K. Magnusson, T. Gudjonsson, *Oncogene* **2016**, *35*, 4244.
[34] M. A. Aleskandarany, E. A. Rakha, M. A. Ahmed, D. G. Powe, E. C. Paish, R. D. Macmillan, I. O. Ellis, A. R. Green, *Breast Cancer Res. Treat.* **2010**, *122*, 45.
[35] a) J. A. Menendez, R. Lupu, *Expert Opin. Ther. Targets* **2017**, *21*, 1001; b) M. E. Monaco, *Oncotarget* **2017**, *8*, 29487.
[36] N. Mori, F. Wildes, T. Takagi, K. Glunde, Z. M. Bhujwalla, *Front. Oncol.* **2016**, *6*, 262.
[37] A. N. Lane, J. Tan, Y. Wang, J. Yan, R. M. Higashi, T. W. M. Fan, *Metab. Eng.* **2017**, *43*, 125.
[38] M. García-Aranda, M. Redondo, *Int. J. Mol. Sci.* **2017**, *18*, 2543.
[39] M. N. Hui, A. Cazet, B. Elsworth, D. Roden, T. Cox, J. Yang, A. McFarland, N. Deng, C.-L. Chan, S. O'Toole, A. Swarbrick, *J. Clin. Oncol.* **2018**, *36*, e24216.
[40] a) F. Yamasaki, D. Zhang, C. Bartholomeusz, T. Sudo, G. N. Hortobagyi, K. Kurisu, N. T. Ueno, *Mol. Cancer Ther.* **2007**, *6*, 2168; b) Y.-K. I. Lau, X. Du, V. Reyannavar, B. Hopkins, J. Shaw, E. Bessler, T. Thomas, M. M. Pires, M. Keniry, R. E. Parsons, S. Cremers, M. Szabolcs, M. A. Maurer, *Oncotarget* **2014**, *5*, 10503.